

Modeling the Atmospheric Circulation and Climatic Conditions over Southern South America During the Late History of the Gondwana Supercontinent

Rosa Hilda Compagnucci

Abstract The different processes responsible for climate and atmospheric circulation forcing and their relevance on the general circulation of the Southern South America together with the conditions over Patagonia, for the period of the Gondwana supercontinent, are identified in this chapter. During the history of this supercontinent, the main paleoclimate forcings were as follows: (1) the continental drift that affected latitude, elevation, and topography; (2) changes in the amount of greenhouse gases in the Earth's atmosphere; and (3) volcanic activity. The paleoatmospheric circulation is analyzed in special sections according to age, Early Triassic to Early Jurassic, Middle to Late Jurassic, and Cretaceous, accordingly with the key changes in the ocean–land distribution and locations of the continents. Different paleoclimatic modeling scenarios through the periods are reviewed and compared with proxy data. From both sources of information, it arises that the opening of the Hispanic Corridor and the formation of the Atlantic Ocean were the chief factors that produced the strong climatic changes registered from the Triassic to the Cretaceous and the remarkable difference with current climate conditions. Other important factors were the variations in the volume of greenhouse gases, especially CO₂, which is related to volcanic activity and changes in the heat transport through the oceans. The observed results suggest that strong monsoon conditions dominated this period of the Gondwana supercontinent. However, there are large differences with respect to the impact of the various climatic forcings between model simulations of circulation general conditions in the Cretaceous. An extensive list of references provides detailed and updated information on the topics covered in this chapter.

Keywords Paleoclimate modeling • Palaeoatmospheric circulation • Forcing of climatic change • Gondwana • Greenhouse gases

R.H. Compagnucci (✉)

DCAO/Facultad de Ciencias Exactas y Naturales, Universidad de Buenos Aires—CONICET,
Guiraldes 2160, Ciudad Universitaria, C1428EGA, Buenos Aires, Argentina
e-mail: rhc@at.fcen.uba.ar

Introduction

Different processes are responsible for climate and atmospheric circulation forcing, and their relevance depends on the specific period analyzed and the frequency of climate change considered. Viewing the Earth's climate as a global system, Frakes (1999) described the evolution of climate throughout the past 600 Ma. He highlighted the complex interactions between the carbon cycle, continental distribution, tectonics, sea-level variation, ocean circulation, and temperature change as well as other processes. Valdes (2000) provided an overview of climatic forcing mechanisms and explored their possible role in Phanerozoic climate variations.

Continental drift and orography are important for low-frequency processes, those involving changes over hundreds of millions of years. Glacial eras characterized times when continental masses were located at the pole due to the capacity of land to support and retain ice sheets. During such periods polar ice caps can maintain themselves and grow through the snow and ice accumulation during repeated annual cycles. Warm climate with Earth free of permanent ice sheets characterized the times when the oceans dominated the polar and subpolar regions of the world and continental masses were located in tropical and subtropical latitudes (Crowley and North 1999).

Forcing through atmospheric greenhouse gases is another important factor of climatic change. Two hundred and fifty million years ago, global CO₂ concentrations were approximately 2,000 ppmv (i.e., 3–8 times higher than today; Royer 2006), producing pronounced warming and enhancing seasonal monsoon circulation. Both forcing processes were present especially during the Triassic and Jurassic periods. These times were characterized by a Gondwana supercontinent without significant landmasses located at the southern polar region, together with exceptionally high CO₂ concentrations. Furthermore, sulfur dioxide (SO₂) is the most voluminous chemically active gas emitted by volcanoes, and the major volcanic eruptions have usually formed sulfuric acid aerosols in the lower stratosphere that cooled the Earth's surface. According to Ward (2009), major volcanic activity in Silicic Volcanic Provinces (SVP) has typically preceded an increase in glaciation and a subsequent decrease in sea level throughout the last 600 Ma.

In this chapter, the influence of the different forcing processes in the Southern South America climate and atmospheric circulation during the Gondwana supercontinent are described.

The paleoatmospheric circulation taken from climatic modeling scenarios through the ages is reviewed and compared with proxy data. Detailed and updated reference information on the relevant topics analyzed in this chapter is provided as well.

Note that the ages indicated for each geological period cited in this chapter correspond to those presented at the US Geological Survey Geologic Names Committee (2010), as Divisions of Geologic Time—major chronostratigraphic and geochronological units.

Forcing Description

Paleoclimatic differences from the Triassic to the Cretaceous periods are due principally to changes in the land–ocean distribution. The Pangaea supercontinent was the largest landmass in the Earth’s history (Fig. 1). According to plate tectonics and continental drift theory, the Pangaea supercontinent began breaking up about 225–200 Ma ago and rifted into two major landmasses during the Jurassic, Laurasia to the north and Gondwana to the south, roughly separated by the equator.

During the Middle to Late Jurassic, new oceanic gateways were formed with, in particular, the opening of the proto-Atlantic Ocean (the so-called Hispanic Corridor) (Fig. 1), connecting the Pacific Ocean to the western Tethys Ocean (Ziegler 1988; Scotese 2001, 2012; <http://www.scotese.com/earth.htm>). The reorganization of the Tethys–Atlantic oceanography was triggered by the opening and deepening of the Hispanic Corridor and produced paleoclimatic changes (Rais et al. 2007).

This single continent stretched in a north–south direction across every part of the zonal atmospheric circulation, thereby producing an extraordinary effect on global paleoclimate (e.g., Dubiel et al. 1991; Sellwood et al. 2000; Valdes 1993; Sellwood and Valdes 2006).

Although the continents have not always been in their present positions, the most extreme land of Southern South America, Patagonia, has always been within latitudes actually affected by the westerlies belt area. Iglesias Llanos et al. (2006) suggested that Patagonia shifted between the Earliest and Late Jurassic from latitudes $\sim 50^\circ$ S to around 30° S affecting its climate (for more details see Volkheimer et al. 2008).

Furthermore, the warm Mesozoic Era (230–65 Ma ago) was likely associated with high levels of CO_2 (Fig. 2) that became stabilized around 2,000 ppm. The Early Jurassic to Late Cretaceous times at 184–66.5 Ma were characterized by very high CO_2 levels (6,000 ppm), though with cool pulses lasting less than 3 Ma (Frakes 1999). Thereafter, CO_2 levels oscillated between very high ($\sim 2,000$ ppm) and low (500 ppm) values (Royer 2006).

A major expansion of Antarctic glaciations starting around 35–40 Ma was likely a response, in part, to declining atmospheric CO_2 levels from their previous peak in the Cretaceous (~ 100 Ma) (DeConto and Pollard 2003). Furthermore, atmospheric CH_4 concentration, land surface albedo, and ocean heat transport may all have played major, but not mutually exclusive, roles (Valdes 2000). Another important factor was the opening of the Drake Passage, between 49 and 17 Ma (Scher and Martin 2006).

Another important influence on climatic change is volcanic activity. It has been suggested that increased volcanic and seafloor-spreading activities during the Jurassic period released large amounts of carbon dioxide—a greenhouse gas—and led to higher global temperatures. In Fig. 3 the data of the major volcanic activity in Silicic Volcanic Provinces (SVP) is presented, together with the average $\delta^{18}\text{O}$ (thick black line) (per million year = 1.45‰ —[per mil]) which represent times of

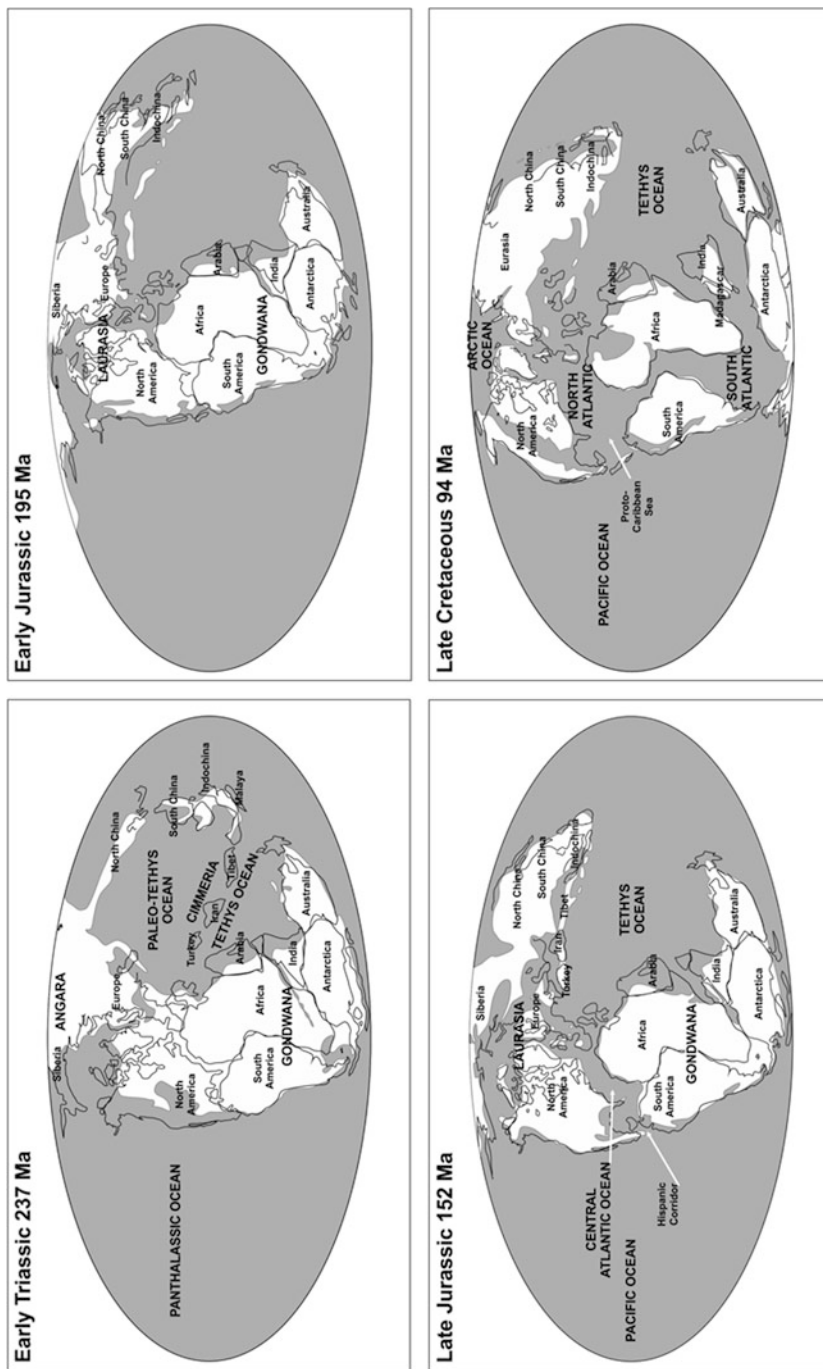


Fig. 1 World map from the Early Triassic (*upper left panel*) to the Late Cretaceous (*lower right panel*) (Adapted from Scotese (2012); <http://www.scotese.com/earth.htm>)

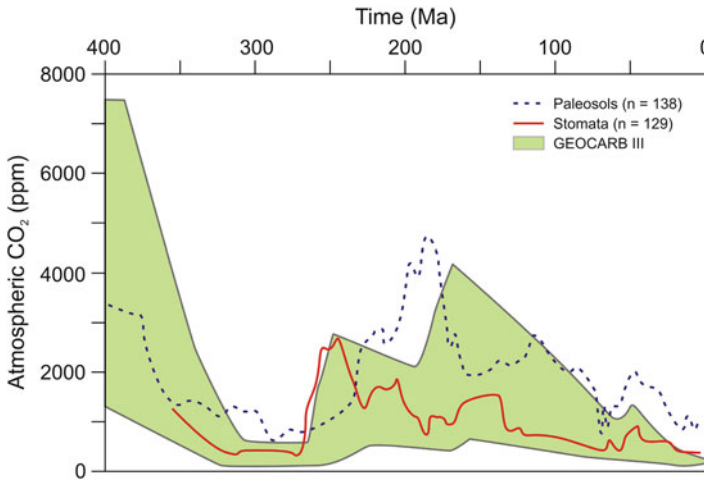


Fig. 2 Atmospheric CO₂ and continental glaciation 400 Ma to present. Plotted CO₂ records represent five-point running averages from each of the four major proxies (Adapted from Royer 2006). Also plotted are the plausible ranges of CO₂ from the geochemical carbon cycle model GEOCARB III (Adapted from Berner and Kothavala 2001). All data have been adjusted to the Gradstein et al. (2004) timescale

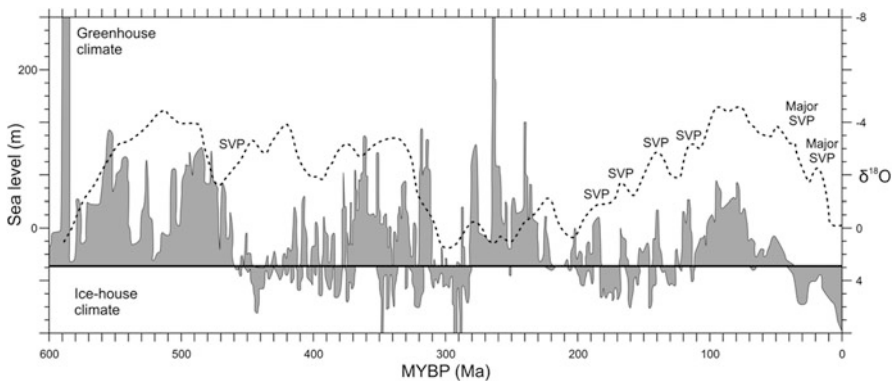


Fig. 3 The times of major volcanic activity in Silicic Volcanic Provinces (SVP). The shaded gray areas show the $\delta^{18}\text{O}$ proxy for tropical sea-surface temperature (From Veizer et al. 1999). Values below the black line show times of glaciation (“icehouse world”), whereas over such line, the values show times of little or no glaciation (“greenhouse world”). The dotted black line shows sea level (Haq et al. 1987; Ross and Ross 1987, 1988; Adapted from Ward 2009)

extensive glaciation or icehouse climate (below the solid back line) or warmer times of limited glaciation or greenhouse climate (above the solid back line) and sea-level oscillations (dotted line). The Gondwana supercontinent began breaking up in the Late Jurassic; the opening of the Atlantic Ocean is coincident with the start of major

SVP. According to Ward (2009), the SVPs, as far back as they have been mapped, typically occurred at the onset of decrease in sea level most likely associated with increased glaciation.

Climate Models of Paleatmospheric Circulations

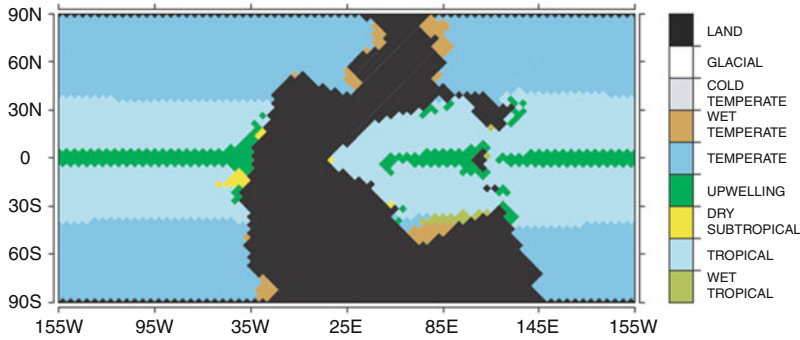
Climate models provide a framework within which existing data can be interpreted and appropriate hypotheses proposed. They are particularly valuable for regions with limited data and provide ways to help interpret local paleoclimate records. Paleatmospheric circulations are normally inferred using three-dimensional general circulation models (GCMs) of the ocean and atmosphere. These models predict the fluid flow on a rotating sphere heated by solar radiation (more information in Crowley and North 1999; Trenberth 1992; Huber et al. 2000; Poulsen 2008, among others). All the different GCM simulations for the Gondwana supercontinent (Moore et al. 1992a, b; Chandler et al. 1992; Valdes and Sellwood 1992; Kutzbach and Gallimore 1989) showed strong seasonal alteration of summer monsoon lows and winter monsoon highs.

Early Triassic to Early Jurassic

In the Middle Permian (Wordian; at ~ 265 Ma ago), the Pangaeian supercontinent was surrounded by a Panthalassa super-ocean, and the CO_2 level was around 1,000+ ppm and remained quite high until the Early Triassic (Royer 2006). Most of Early Jurassic atmospheric simulations show the dominance of monsoonal circulation conditions along the eastern part of Pangaea (Scotese and Summerhayes 1986; Crowley et al. 1989; Kutzbach and Gallimore 1989; Kutzbach et al. 1990; Fawcett et al. 1994; Barron and Fawcett 1995).

The sensibility of the Wordian climate to changes in greenhouse gas concentrations, high-latitude geography, and Earth orbital configurations was analyzed by Winguth et al. (2002) using a coupled atmosphere–ocean model. The $1\times \text{CO}_2$ concentration (present level) would more likely be associated with a glacial climate, whereas high CO_2 ($8\times \text{CO}_2$) concentrations simulate very warm conditions, even in high latitudes.

The simulated climate with $4\times \text{CO}_2$ present level (Fig. 4) usually agrees well with sediments and phytogeographical patterns and has a significantly warmer polar climate than the present day, owing to increased flux of heat from ocean to atmosphere in high latitudes. The simulated ocean conditions is characterized by the following: a strong westward equatorial current which is blocked by islands at the eastern Tethys Sea, a warm poleward-directed currents along the Tethys coast and east coast of Gondwana, a cold equatorward current along the east coast of Angara, large meridional overturning circulation cells with deep water formation at



Climate Zone	Water Mass Essentials	Geological Recognitions
Glacial	Surface permanent frozen; SST < -1.8°C	Marine till
Cold temperate	Winter ice flows; SST -1.8 – 0°C	Dropstones, rhythmites
Wet temperate	Brackish surface water; SST 0 – 20°C, salinity < 32	Temperate peats, organic rich shales
Temperate	Mixed water column; SST 0 – 20°C, salinity 32–37	Clastics
Cool subtropical	Upwelling currents; vertical velocity $w > 1 \times 10^{-6} \text{ m s}^{-1}$	Organic-rich shales, phosphorites, cherts
Dry subtropical	High evaporation; salinity > 37	Gypsum, halite, sabkha facies
Tropical	Deep light penetration; SST > 20°C, salinity 32–37	Carbonates, oolites, coralgal reefs
Wet tropical	High precipitation or continental runoff; SST > 20°C, salinity < 32	Tropical peats, muddy sediments

Fig. 4 Water mass classification according to Ziegler et al. (1998) derived from the climate simulation with $4 \times \text{CO}_2$ concentrations (Winguth et al. 2002)

both poles, and a warm deep ocean with low current speed in the eastern equatorial Panthalassa. The simulations suggest that a moderate climate over South Gondwana could be reproduced by an atmospheric CO_2 concentration of at least four times present levels and/or the existence of a south polar seaway that further increases the heat flux to the atmosphere from the ocean.

The climate of the Late Permian and Triassic times (~250–200 Ma) has been described in terms of strong continental climate conditions and monsoons. The paleoclimate conditions were simulated by Kutzbach and Gallimore (1989) using idealized Pangaeon continent with changes in CO_2 and solar luminosity. In spite of

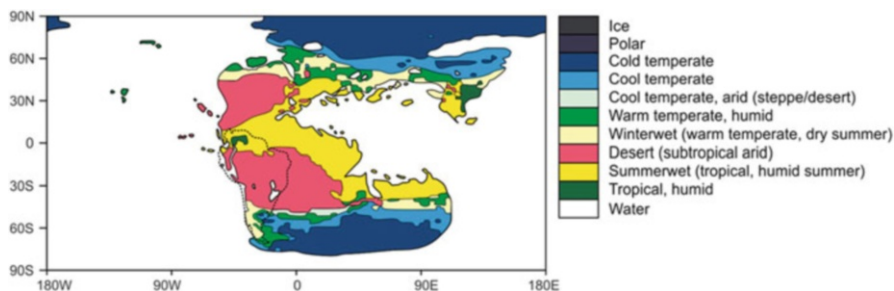


Fig. 5 Following Walter (1985), the biome zones for the Late Triassic based on the model predicted temperatures and precipitation are shown. At the *right*, the key to Walter's (1985) biome zones (Adapted from Sellwood and Valdes 2006)

the various limitations of the simulations carried out by these authors, the resulting scenarios show the mechanism whereby the large Pangaeian continent produces the conditions needed for massive summer and winter monsoonal circulations and cross-equatorial flows. The presence of the large continent also helps to produce the high summer temperatures and evaporation rates and the long overland trajectories that deplete the available atmospheric moisture. Acting together, these factors generate the large arid region in the continental interior and in the equatorial zone. The presence of the large continent also helps to produce the very cold winters of middle and high latitudes and the very hot summers of the tropics.

Sellwood and Valdes (2006) simulated the climate responses to the Mesozoic changes in geography. For the Triassic period, the Central Pacific (Panthalassa) is modeled as having a super, and semipermanent, El Niño system.

Figure 5 shows the biome zones according to the precipitation, temperature, and evaporation model simulated. Southwestern Gondwana is winter-wet. The eastern parts of Gondwana are moister than the western parts, being generally wetter during the summer months (particularly December, i.e., a modeled summer-wet biome/climate). The balance between evaporation and precipitation reflects these seasonal changes. Southern Gondwana is in balance, or has an excess of evaporation, from November through February (summer dryness). But from March to October, the southern parts of the continent in particular have an excess of precipitation (winter-wet). This embraces the months of winter darkness for the southern polar area.

In the Early Jurassic three-dimensional model simulation of Chandler et al. (1992), the atmospheric composition, solar radiation, and orbital parameters were set at present-day values. The resulting major features include warm surface-air temperatures, extreme continental aridity in the low and middle latitudes of western Pangaea, and monsoons which dominate along the midlatitude coast of Tethys and Panthalassa and also affect conditions deep into the continental interiors in some regions. They also experimented with variations in topography, sea-surface temperature, vegetation, and CO₂ content and discovered that none of the scenarios yielded continental interiors in which winter temperatures remained above freezing

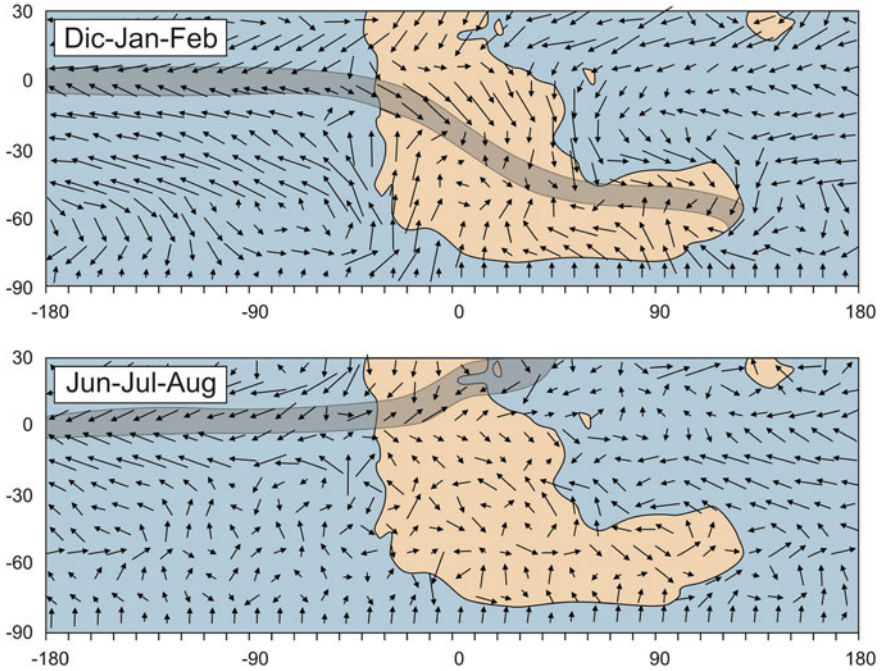


Fig. 6 Simulated global distribution of Early Jurassic wind vectors (a) surface wind; hatched line indicates approximate position of ITCZ for the South Hemisphere summer (Dec–Jan–Feb) and South Hemisphere winter (Jun–Jul–Aug) (Adapted from Chandler et al. 1992)

everywhere. The most important outcome of the simulations is that the warm climate of the Early Jurassic could be maintained without additional forcing from CO_2 . The results show that increased ocean heat transport may have been the primary force generating warmer climates during the past 180 Ma. The mega-monsoons are found to be associated with localized pressure cells whose positions are controlled by topography and coastal geography. The simulated sea-level pressure (not shown) and surface winds (Fig. 6) shown in the Southern Hemisphere, as in the Northern Hemisphere, pressure centers localized above high topography regions, the winter high-pressure cells being shifted poleward from the summer lows. During winter the winds are generally light and below freezing surface-air temperature extends across most of the southern Pangaea, although seasonally averaged coastal temperatures remain above freezing at all latitudes. During summer, monsoon circulations are responsible for increases in Southern Hemisphere precipitation. Cyclonic circulation about the subtropical low in the southwestern Pangaea causes surface winds over the western Tethys Ocean to flow southward, where they invade upon Pangaea in the region of the Indian subcontinent. Winds from the polar oceans, despite their cooler source, also cause prominent summer precipitation maximum over southeastern Pangaea, primarily as a result of the uplift of air over

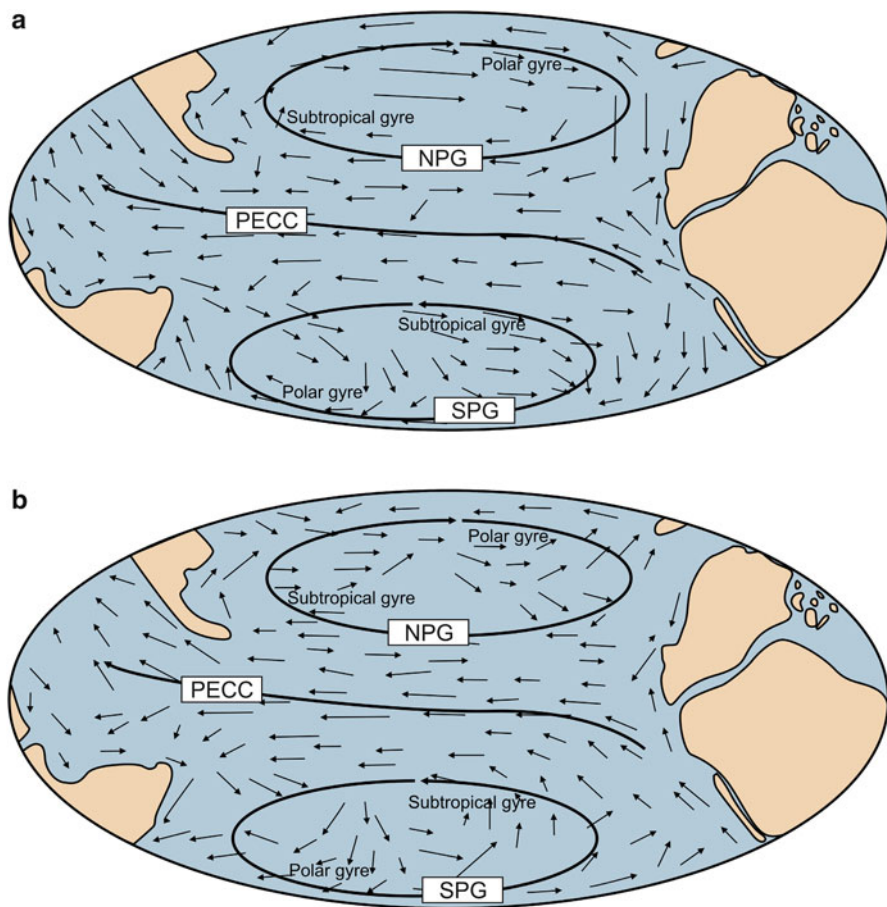


Fig. 7 Schematic representation of the surface oceanic circulation in the Panthalassa Ocean for the Northern Hemisphere **(a)** winter monsoon and **(b)** summer monsoon: Panthalassa Equatorial Counter Current (*PECC*); North Panthalassa Gyre (*NPG*) and South Panthalassa Gyre (*SPG*) or South Central Gyre (Adapted from Arias 2008)

coastal mountains. This monsoon circulation causes great seasonal variations in the Southern Hemisphere precipitation fields.

The surface oceanic circulation during the Early Jurassic Panthalassa oceans modeled by Arias (2008) is shown in Fig. 7. The proposed conceptual paleoceanographic model was based on fundamental physical–oceanographic principles, a global paleogeographic reconstruction, the atmospheric wind paleo-patterns, and paleobiogeographic data. The resulting Panthalassic oceanic circulation pattern presents approximately hemispherical symmetric structure of two large subtropical gyres that rotates clockwise in the Northern Hemisphere and anticlockwise in the Southern Hemisphere. During the Northern Hemisphere summer, the surface Tethyan Ocean circulation is dominated by monsoonal westerly directed equatorial

surface currents that reached its western corner and drove them to the north, along the northern side of the Tethys Ocean, and in opposite direction during the winter.

Middle and Late Jurassic

In the Middle to Late Jurassic the Hispanic Corridor (Fig. 1), connecting the Pacific Ocean to the western Tethys Ocean, affected the paleo-oceanic currents permitting a globe-circling, mainly west-flowing current system in low latitudes (Winterer 1991; Rais et al. 2007) and consequently the atmospheric circulation mainly in the tropical regions.

Moore et al. (1992a, b) used a GCM to obtain two Kimmeridgian/Tithonian (~154.7–145.6 Ma) paleoclimate seasonal simulations, with geologically inferred paleotopography: one simulation used a CO₂ concentration of 280 ppm (preindustrial level) and the other used 1,120 ppm. Increasing the CO₂ content fourfold, it warms virtually the entire planet.

The simulations show greatest warming over the higher-latitude oceans and a smaller one over the equatorial and subtropical regions (Fig. 8). During the Southern Hemisphere summer (Fig. 8c), latitudes north of 30° S were characterized by the influence of the Intertropical Convergence Zone (ITCZ), while southwestern South America was dominated by the movement of the Southern Panthalassa ocean semipermanent anticyclone, which shifted to the south, affecting the southwest margins of Gondwana, that is, Patagonia. The monsoon lows were centered poleward of the western Tethys Sea, near 35° S. This location is just east of the region of summer maximum temperature. The wind pattern over Patagonia for June to August was opposite to that during summer. During winter the Panthalassa subtropical high was centered near 25° S. South of it, a subpolar low, centered near 60° S, dominated the south Panthalassa Ocean. These high- and low-pressure systems along with the continental winter monsoon high, which was located poleward of the western Tethys Sea and was centered near 40° S, were responsible for the winds from the northwest (Fig. 8d), forcing advection of wet and warm air over Patagonia. Furthermore, in the middle troposphere the axes of the Southern Hemisphere midlatitude storm track are located over 60° S. These factors are related to high positive net precipitation where precipitation exceeds evaporation. The model-simulated precipitation rate in the region is ≥ 5 mm/day (Valdes 1993) in concordance with the coal localities that are proxies for wet environments (Scotese 2012).

Moore et al. (1992a) proposed that the Jurassic warmth suggested by climate proxies may be explained by elevated atmospheric CO₂. In contrast, Chandler et al. (1992), for the Early Jurassic simulation, suggested that the resulted warm SSTs in energy balance without high atmospheric CO₂ imply that a warm Jurassic climate could have been the product of enhanced poleward heat transport through the oceans.

In other words, two feedback mechanisms are presumed to be primarily responsible for the very warm climate over Patagonia during the Jurassic: the elimination of sea and land ice that resulted from the warm polar sea-surface temperatures (SSTs) and the equatorward shift of Antarctica resulting in a decrease in surface albedo.

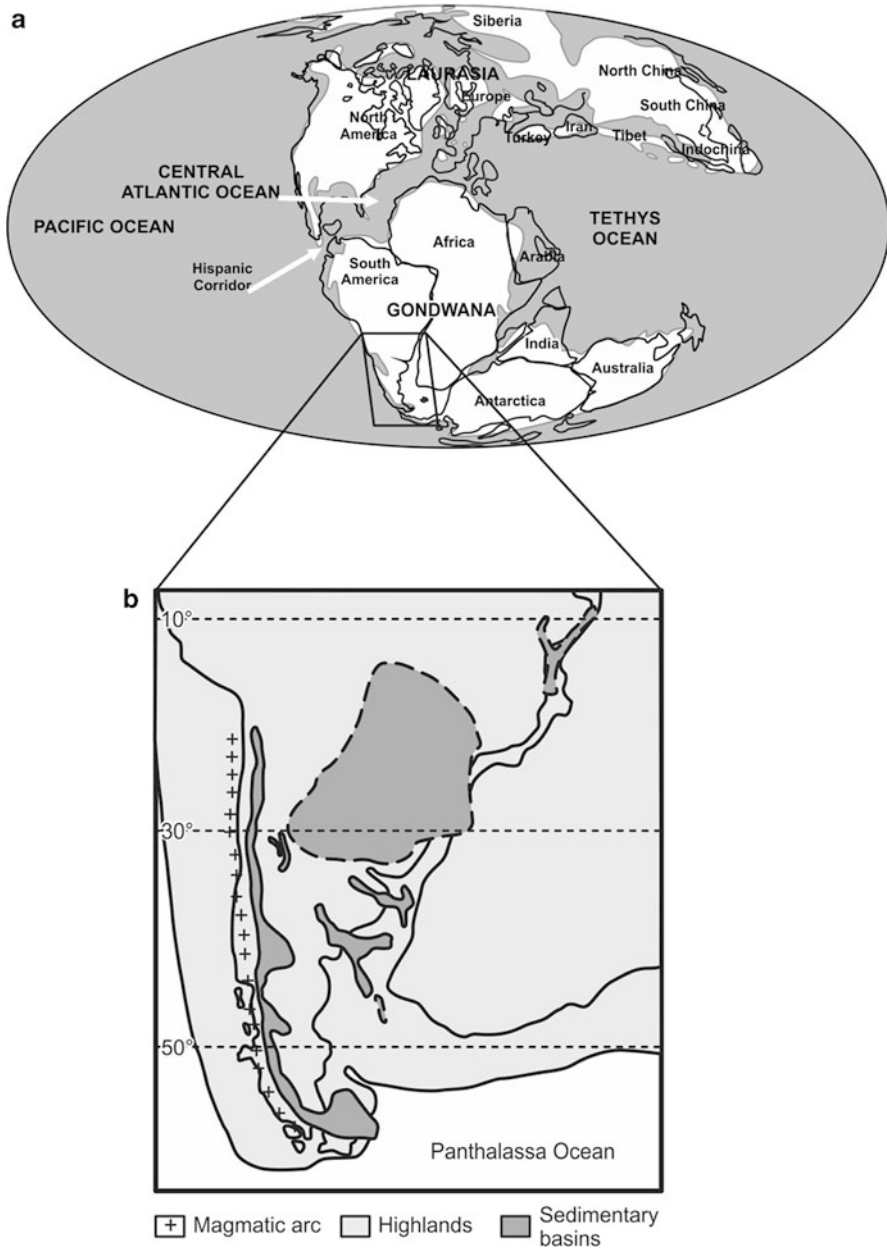


Fig. 8 Latest Jurassic–Earliest Cretaceous: (a) Paleolatitude and paleogeography (Adapted from Scotese 2012); (b) Paleogeographic map of the southwestern Gondwana continent (Adapted from Scherer and Goldberg 2007) and maps of simulated Kimmeridgian/Tithonian surface wind vectors using 1,120 ppm CO₂ for (c) December, January, and February; (d) June, July, and August (Adapted from Moore et al. 1992a)

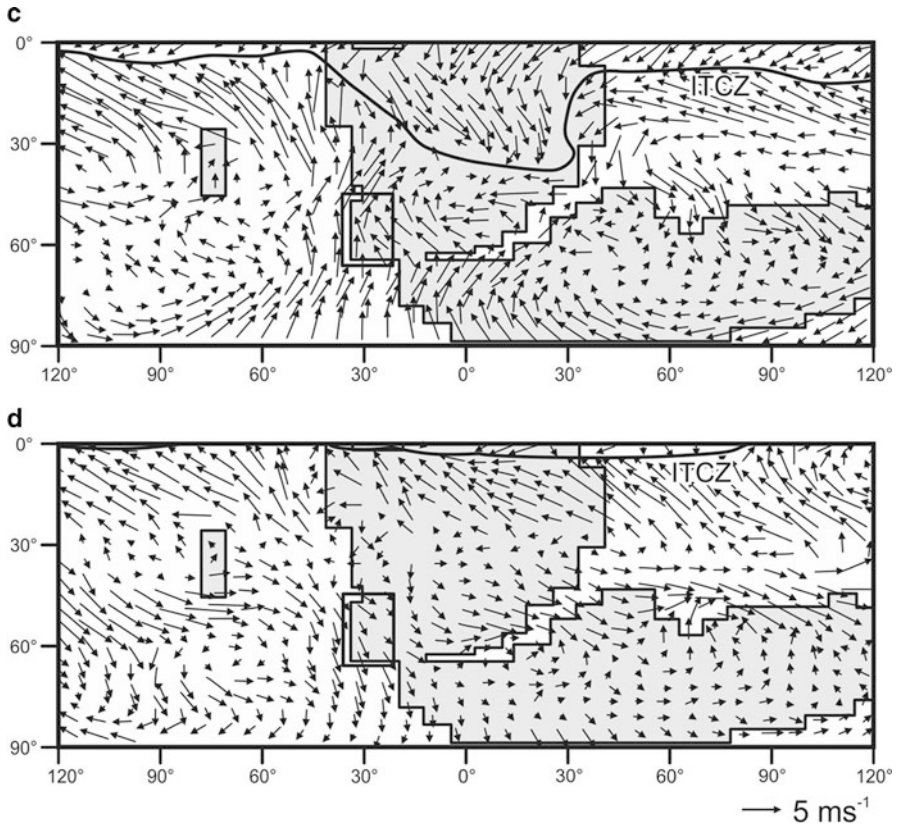


Fig. 8 (continued)

The modeled Kimmeridgian climate of Sellwood and Valdes (2006), between about 10° and 30° S, shows evaporation exceeding precipitation and a return to excess precipitation in the mid-to-high southern latitudes (Fig. 9). From fossil evidence, Jurassic plant productivity and maximum diversity were concentrated at mid-latitudes, reflecting a migration of the zone of peak productivity from low to higher latitudes during greenhouse times (reviewed and modeled in Rees et al. 2000).

Cretaceous

During the Late Jurassic to Early Cretaceous times, the separation between Gondwana and Laurasia was already well in progress, and the South Atlantic Ocean had already started to develop between those continents. India separated from Madagascar and raced northward on a collision course with Eurasia. North America

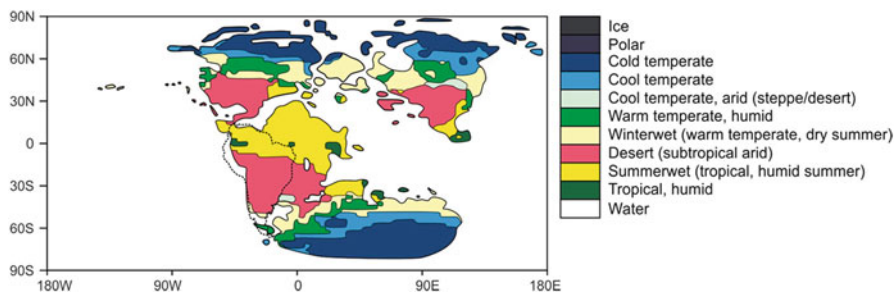


Fig. 9 The Walter's (1985) biome zones for the Late Jurassic (Kimmeridgian) based on the model predicted temperatures and precipitation (Adapted from Sellwood and Valdes 2006)

was connected to Europe, and Australia was still joined to Antarctica. By the Late Cretaceous, the oceans had widened, and India approached the southern margin of Asia (see Scotese 2012).

The Early Cretaceous was a mild “icehouse” world. There was snow and ice during the winter seasons, and cool-temperate forests covered the polar regions. The Late Cretaceous was instead characterized by super greenhouse intervals of global warmth with ice-free continents. Globally averaged surface temperatures were 6–14 °C higher than at present (Barron 1983), and the temperature gradient between the poles and the equator was lower than today, that is, about 50 °C in the Northern Hemisphere and 90 °C in the Southern Hemisphere. The difference is largely due to adiabatic cooling reflecting the elevation of Antarctica. Frakes (1999) summarized the data on estimates of Cretaceous sea-surface and terrestrial temperatures.

There are four different assumptions concerning Cretaceous temperatures and meridional gradients: (1) tropical sea-surface temperatures were the same as today, but polar temperatures were warmer (5–8 °C) except when ice was present (0–5 °C); (2) the tropics were significantly cooler and midlatitudes warmer than today; (3) tropical sea-surface temperatures were 32–34 °C, with polar regions 10–18 °C; and (4) tropical sea-surface temperatures were about 42 °C and polar temperatures >18 °C. Furthermore, different hypothesis can explain the drastic warming and equable high latitudes during super-greenhouse intervals of the Cretaceous and Early Cenozoic. On the basis of coupled ocean–atmosphere model simulations of the Middle Cretaceous, Poulsen et al. (2003) hypothesized that the formation of an Atlantic Gateway could have contributed to the Cretaceous thermal maximum. Kump and Pollard (2008), by simulating the Middle Cretaceous using 4× CO₂ from preindustrial atmospheric level, failed to produce results to explain the extreme high-latitude warmth implied by temperature proxy data. However, simulations with the combined increases in cloud droplet radii, which mainly affect cloud optical depth, and precipitation efficiency, resulted in a reduction in global cloud cover from 64 to 55 % with optically thinner clouds which reduced planetary albedo from 0.30 to 0.24. The ensuing warming was dramatic, both in the tropics and in high latitudes, where warming was augmented by surface albedo. In other words, warming was

produced by albedo reduction due to diminishing cloud cover. Then, surface albedo feedback augmented warming in the tropics and high latitudes and produced almost the vanishing of snow and sea-ice cover, thus forcing less albedo and more intense warming. Otto-Bliesner et al. (2002) altered the models by the inclusion of high-latitude forest thus changing the paleogeography. These low-albedo forests warmed the high-latitude continents, which then transferred more heat to the high-latitude oceans, impeding sea-ice formation and warming coastal regions.

The scenarios for the Turonian (~93.5–89.3 Ma) paleogeography were obtained by Floegel (2001) using GCM simulations with different orbital configurations and 1,882 ppm CO₂ (5× AD 2,000 CO₂, 7× preindustrial CO₂) concentrations (Fig. 10). The simulated atmospheric circulation resulted in a much more complex circulation than that observed today. In this model, the tropical easterlies remain constant and strong throughout the year. However, at higher latitudes the circulation varies with the seasons. Due to the absence of polar highs during the winter, strong westerly wind belts develop between 50° S and the high-pressure zones at 30° S. Another important difference in Floegel's scenarios lies in the strong trade winds, which developed during each hemispheric winter.

In Floegel's model, in the Southern Hemisphere summer (December to February), the polar region is under the influence of a low atmospheric pressure system, and therefore the westerly winds were weak and variable and may have even had a reverse direction. Also, the subtropical to polar frontal systems would not exist (Fig. 10). This would result in disruption of the mid- and high-latitude wind systems. In the winter (June to August), the southern polar region is under the influence of a high-pressure system and the westerlies are well developed (Hay et al. 2005; Hay 2008).

The Maastrichtian (65.5–70.6 Ma) paleowind scenario in Fig. 11 was obtained by Bush (1997) using an atmospheric–oceanic GCM, dynamically and thermodynamically coupled, with four times the present-day value of atmospheric CO₂, as indicative of Cretaceous levels. Even with these relatively new results, it is necessary to be cautious with the adopted paleogeographic reconstruction for the Maastrichtian (Ziegler et al. 1982), which was used in the model, if the Drake Passage were considered as it was already open.

Some GCM simulations of the Cretaceous super-greenhouse also considered as a boundary condition that the Drake Passage was already open (Sewall et al. 2007; Poulsen et al. 2007; Kump and Pollard 2008; Zhou et al. 2008; among others), while others considered that the Drake Passage was still closed (e.g., Haywood et al. 2004). For instance, Bush and Philander (1997) had estimated a later age for the opening of the Drake Passage, ranging from 49 to 17 Ma ago; see also more details and additional references in Cavallotto et al. (2011).

The earliest connection between the Pacific and Atlantic oceans at the Drake Passage is still controversial but very important, because the gateway opening probably had a profound effect on the global circulation and climate (see Cavallotto et al. 2011). The Drake Passage influence on climate was studied by Sijp and England (2004) by means of three main model simulation experiments, all of them set up identically with the exception of bathymetric data. They either kept (a) the

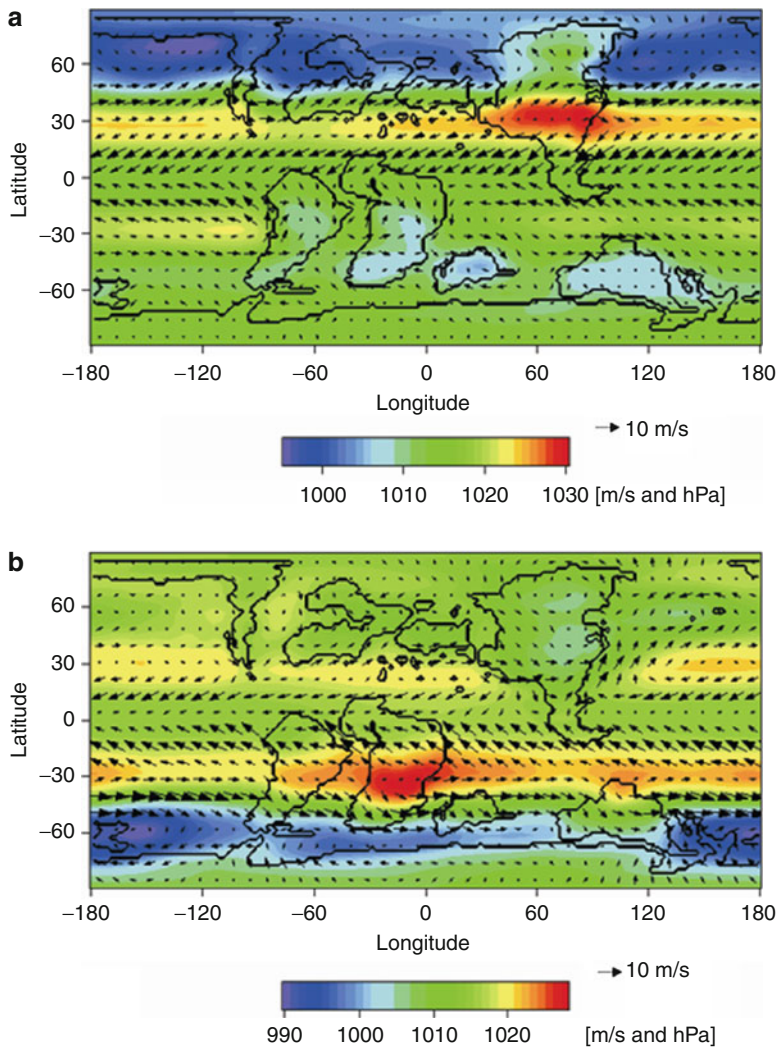


Fig. 10 Turonian (93.5 Ma) wind speed and pressure at sea level for (a) Dec, Jan, Feb and (b) Jun, Jul, Aug [m/s and hPa] (From Floegel 2001; © Sascha Floegel, IFM-GEOMAR, Kiel, Germany)

Drake Passage closed by a land bridge between the Antarctic Peninsula and South America, (b) the Drake Passage open to a maximum depth of 690 m, or (c) the Drake Passage open at its present-day depth, which was modeled as an uninterrupted through flow at a depth of ca. 2,316 m.

The modeled climate with the Drake Passage closed is characterized by warmer Southern Hemisphere surface-air temperature and little Antarctic ice. An increase in Antarctic sea ice and a significant cooling of the Southern Hemisphere would have

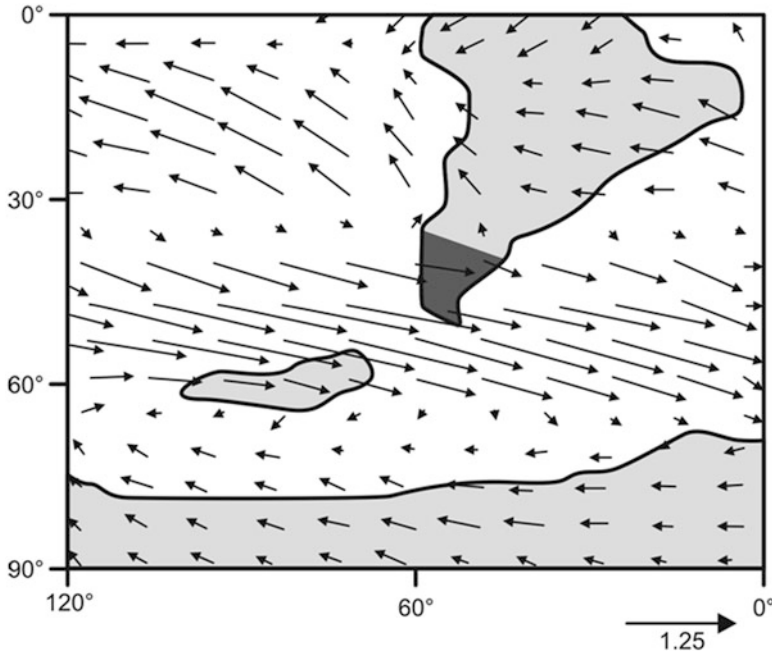


Fig. 11 Annual mean wind stress vectors (in dynes per square centimeter) for the Late Cretaceous. Arrows are scaled as displayed in the *bottom right* (Adapted from Bush 1997)

taken place when the Drake Passage was open to a much shallower depth of 690 m. As the Drake Passage opened, the climate would have become mostly similar in the Southern Hemisphere to the conditions of the Drake Passage if open at 690 m.

Bush's (1997) simulated pattern of annual mean wind stress (Fig. 11) resulted in a pattern similar to that of the present day with only some changes as a consequence of the modified continental–ocean distribution. The annual mean fields show the tropical–subtropical region circulation characterized by the ITCZ and the easterly winds occupying the latitudinal band from 30° S to 30° N. The Southern Hemisphere westerlies occupy the latitudinal band from 40° to 70° S and the midlatitude tropospheric jets dominate the atmospheric circulation over Patagonia (Fig. 11). The simulation shows no poleward shift of the midlatitude westerlies in response to an ice-free planet.

In the Bush and Philander's (1997) simulation, using a coupled atmosphere–ocean GCM with quadrupled CO₂, the annual mean Hadley circulation indicates a general reduction in strength of the Southern Hemisphere cells in the Cretaceous, with the south equatorial Hadley cell weakening by 20%. Subsidence in the high southern latitudes decreased dramatically in the Cretaceous in response to the elimination of the Antarctic ice sheet, which in the present climate induces strong subsidence poleward of 75° S. As a consequence, the strengths of the middle- and high-latitude cells decrease. In addition, the separation of the North and South

American continents allowed stronger northeasterly trades flowing from the Tethys basin into the Pacific Ocean basin, whereas the strength of the southeasterly winds off the western coast of South America remains approximately the same.

Both modeling analysis, Bush and Philander's (1997) and Hotinski and Toggweiler's (2003), suggest the possibility of intensified surface circulation. The stronger upper tropospheric westerlies and stronger lower tropospheric easterlies over the tropical Pacific Ocean suggest a "permanent El Niño" state, as Davies (2006) found by analyzing laminated sediments. The model results showed the global precipitation approximately 10 % higher than at present. The mean annual temperatures increased and the amplitude of seasonal cycle in near-surface temperatures diminished, consequently precluding the presence of year-round snow or ice in the simulation. In high latitudes, however, there are regions that seasonally drop below freezing.

Conclusions

A major transformation in the global paleogeography occurred between the Triassic and the Cretaceous, which involved opening of the Hispanic Corridor and formation of the Atlantic Ocean. These are the main factors that produced the climatic changes registered in this period. Other important factors were the variations in the greenhouse gases, especially in CO₂ which is related to the volcanic activity and the heat transport through the oceans. Strong monsoon conditions dominated during the Mesozoic in the Gondwana supercontinent.

The major climate features of the Early Jurassic, as simulated by means of GCM, comprised warm surface-air temperatures, extreme continental conditions in the low and midlatitudes, and monsoonal environments, which basically dominated along the midlatitude coasts of the Tethys and the Panthalassa oceans. The sea-level pressures over the continent show high-pressure cells during winter and opposite low pressure in summer.

Over the oceans, a dipole of subpolar low-pressure cells and subtropical high-pressure zone is present. Despite the similarity between the hemispheric patterns, a substantial degree of asymmetry is caused by land-sea distribution and topographic differences. The strong differences between winters and summers generated a large annual cycle. During the Southern Hemisphere winter, faint insolation and strong heat loss caused a decrease of the temperature over the interior of the southern Pangaea, and consequently, the sinking cooled air could create a high-pressure belt over the Gondwana continent. At the same time during the Northern Hemisphere summer, the warm temperatures can also generate an extensive low-pressure zone over central Laurasia, northeastern Pangaea, (between 10° N and 30° N) that deepens above the higher elevations in the eastern part of the continent. In the Southern Hemisphere winter, the situation was exactly the inverse.

In the Cretaceous greenhouse world, the paleogeography was dramatically different from that of the Gondwana continent, which was by now breaking up

and when the Atlantic Ocean was already well developed. Results from a coupled ocean–atmosphere model indicate that the opening of the Atlantic Equatorial Gateway could have caused a large-scale reorganization of the tropical climate and regional warming. This mechanism was considered as a cause of the Cretaceous Thermal Maximum. Both the oceanic and atmospheric circulation was affected. The westerly winds developed only seasonally. In the absence of persistent westerlies, the subtropical ocean gyres would have weakened leading to an ocean circulation dominated by eddies. As a result, the pycnocline would have been more diffuse than today, contributing to enhanced thermohaline circulation and global oceanic heat transport (Hay 2008).

A caution note must be highlighted about the very large differences in the response of the general circulation models to Cretaceous boundary conditions. For example, the GENESIS model (Bice et al. 2006) must have had much higher pCO₂ than previously thought (~12 × present-day levels) to match the warmest tropical paleotemperature. Otherwise, high atmospheric pCO₂ levels are not required to achieve a very warm Cretaceous climate. With moderate pCO₂ levels (~3 × present-day levels), the Hadley coupled ocean–atmosphere model predicts a hot Cretaceous world dominated by latent heat (Markwick and Valdes 2002; Haywood et al. 2004). The NCAR model with moderate pCO₂ levels (~3 × present-day levels) predicts deep-ocean temperatures of 9–11 °C and surface temperatures that are 3–4 and 6–14 °C warmer than modern at low and high latitudes, respectively. Ocean heat transports in the model are diminished in the Northern Hemisphere and enhanced in the Southern Hemisphere (Otto-Bliesner et al. 2002). A similar spectrum of climate models used for the Cretaceous is being used to predict future climates, each of them with different sensitivity to increased greenhouse gas concentration.

In summary, the climate of the Gondwana supercontinent was quite varied and significantly different from present-day conditions in most of it. Very high mean annual temperatures and increased precipitation characterized the climate of the second half of the Mesozoic, which have had strong influence in the landscape and ecosystem evolution.

References

- Arias C (2008) Palaeoceanography and biogeography in the Early Jurassic Panthalassa and Tethys Oceans. *Gondwana Res* 14:306–315
- Barron EJ (1983) A warm, equable Cretaceous: the nature of the problem. *Earth Sci Rev* 19:305–338
- Barron EJ, Fawcett PJ (1995) The climate of Pangaea: a review of climate model simulations of the Permian. In: Scholle PA, Peryt TM, Ulmer- Scholle DS (eds) *The Permian of Northern Pangea*, vol 1. Springer, Berlin, pp 37–52
- Berner RA, Kothavala Z (2001) GEOCARB III: a revised model of atmospheric CO₂ over phanerozoic time. *Am J Sci* 301:182–204
- Bice KL, Birgel D, Meyers PA, Dahl KA, Hinrichs K, Norris RD (2006) A multiple proxy and model study of Cretaceous upper ocean temperatures and atmospheric CO₂ concentrations. *Paleoceanography* 21, PA2002. doi:[10.1029/2005PA001203](https://doi.org/10.1029/2005PA001203)

- Bush ABG (1997) Numerical simulation of the Cretaceous Tethys circumglobal current. *Science* 275:807–810
- Bush ABG, Philander SGH (1997) The late Cretaceous: simulation with a coupled atmosphere–ocean GCM. *Paleoceanography* 21:475–516
- Cavallotto JL, Violante RA, Hernández-Molina FJ (2011) Geological aspects and evolution of the Patagonian continental margin. *Biol J Linn Soc* 103:346–362
- Chandler M, Rind D, Ruedy R (1992) Pangean climate during the Early Jurassic: GCM simulations and the sedimentary record of paleoclimate. *Bull Geol Soc Am* 104:543–559
- Crowley TJ, North GR (1999) *Paleoclimatology*. Oxford University Press, New York, 360 pp
- Crowley TJ, Hyde WT, Short DA (1989) Seasonal cycle variations on the supercontinent of Pangea. *Geology* 17:457–460
- Davies A (2006) High resolution palaeoceanography and palaeoclimatology from mid and high latitude Late Cretaceous laminated sediments. Unpublished doctoral dissertation, Faculty of Engineering Science and Mathematics, School of Ocean and Earth Science, University of Southampton, Southampton, 274 pp
- DeConto RM, Pollard D (2003) Rapid Cenozoic glaciation of Antarctica induced by declining atmospheric CO₂. *Nature* 421:245–249
- Dubiel RF, Parrish JT, Parrish JM, Good SC (1991) The Pangaean megamonsoon—evidence from the Upper Triassic Chinle Formation, Colorado Plateau. *Palaeos* 6:347–370
- Fawcett PJ, Barron EJ, Robison VD, Katz BJ (1994) The climatic evolution of India and Australia from the Late Permian to Mid-Jurassic: a comparison of climate model results with the geologic record. *Geol Soc Am Spec Pap* 288:139–158
- Floegel S (2001) On the influence of precessional Milankovitch cycles on the Late Cretaceous climate system: comparison of GCM-results, geochemical, and sedimentary proxies for the Western Interior Seaway of North America. *Universitätsbibliothek der Christian-Albrechts-Universität Kiel, Kiel*
- Frakes LA (1999) Estimating the global thermal state from Cretaceous sea surface and continental temperature data. *Spec Pap-Geol Soc Am*: 49–58
- Gradstein F, Ogg J, Smith A, Bleeker W (2004) A new Geologic Time Scale, with special reference to Precambrian and Neogene. *Episodes* 27:83–100
- Haq BU, Hardenbol J, Vail PR (1987) Chronology of fluctuating sea levels since the Triassic (250 million years ago to present). *Science* 235:1156–1167
- Hay WW (2008) Evolving ideas about the Cretaceous climate and ocean circulation. *Cretac Res* 29(5–6):725–753
- Hay WW, Flögel S, Söding E (2005) Is the initiation of glaciation of the Cretaceous Ocean–Climate System on Antarctica related to a change in the structure of the ocean? *Glob Planet Change (Geol Soc Am Spec)* 45:23–33
- Haywood AM, Valdes PJ, Markwick PJ (2004) Cretaceous (Wealden) climates: a modeling perspective. *Cretac Res* 25:303–311
- Hotinski RM, Toggweiler JR (2003) Impact of a Tethyan circumglobal passage on ocean heat transport and “equable” climates. *Paleoceanography* 18(1):1007. doi:[10.1029/2001PA000730](https://doi.org/10.1029/2001PA000730)
- Huber BT, MacLeod KG, Wing SL (eds) (2000) *Warm climates in earth history*. Cambridge University Press, Cambridge, p 462
- Iglesias Llanos MP, Riccardi AC, Singer SE (2006) Palaeomagnetic study of Lower Jurassic marine strata from the Neuquén Basin, Argentina: a new Jurassic apparent polar wander path for South America. *Earth Planet Sci Lett* 252:379–397
- Kump LR, Pollard D (2008) Amplification of Cretaceous warmth by biological cloud feedbacks. *Science* 320:195
- Kutzbach JE, Gallimore RG (1989) Pangaean climates: megamonsoons of the megacontinent. *J Geophys Res* 94(D3):3341–3357. doi:[10.1029/JD094iD03p03341](https://doi.org/10.1029/JD094iD03p03341)
- Kutzbach JE, Guetter PJ, Washington WM (1990) Simulated circulation of an idealized ocean for Pangaean time. *Paleoceanography* 5(3):299–317

- Markwick PJ, Valdes PJ (2002) A quantitative evaluation and application of the results of a Maastrichtian (Late Cretaceous) coupled ocean–atmosphere experiment using the HadCM3 AOGCM, Cretaceous Climate and Oceans Dynamics Workshop, 14–17 July 2002, The Nature Place, Florissant, CO, USA
- Moore GT, Hayashida DN, Ross CA, Jacobson SR (1992a) Palaeoclimate of the Kimmeridgian/Tithonian (Late Jurassic) world. I. Results using a general circulation model. *Palaeogeogr Palaeoclimatol Palaeoecol* 93:113–150
- Moore GT, Sloan LC, Hayashida DN, Umrigar NP (1992b) Paleoclimate of the Kimmeridgian/Tithonian (Late Jurassic) world. II. Sensitivity tests comparing three different paleotopographic settings. *Palaeogeogr Palaeoclimatol Palaeoecol* 95:229–252
- Otto-Bliessner BL, Brady EC, Shields C (2002) Late Cretaceous ocean: coupled simulations with the National Center for Atmospheric Research Climate System Model. *J Geophys Res* 107. doi:10.1029/2001JD000821
- Poulsen CJ (2008) Paleoclimate modeling, pre-Quaternary. In: Gornitz V (ed) *Encyclopedia of paleoclimatology and ancient environments*. Kluwer Academic, Dordrecht, pp 700–709
- Poulsen CJ, Gendaszek AS, Jacob R (2003) Did the rifting of the Atlantic Ocean cause the Cretaceous thermal maximum? *Geology* 31:115–118
- Poulsen CJ, Pollard D, White TS (2007) General circulation model simulation of the $\delta^{18}\text{O}$ content of continental precipitation in the middle Cretaceous: a model-proxy comparison. *Geology* 35:199–202
- Rais P, Louis-Schmid B, Bernasconi SM, Weissert H (2007) Palaeoceanographic and palaeoclimatic reorganization around the Middle-Late Jurassic transition. *Palaeogeogr Palaeoclimatol Palaeoecol* 251:527–546
- Rees PM, Zeigler AM, Valdes PJ (2000) Jurassic phytogeography and climates: new data and model comparisons. In: Huber BT, MacLeod KG, Wing ST (eds) *Warm climates in earth history*. Cambridge University Press, Cambridge, pp 297–318
- Ross CA, Ross JRP (1987) Late Paleozoic sea levels and depositional sequences. In: Ross CA, Haman D (eds) *Timing and depositional history of eustatic sequences: constraints on seismic stratigraphy*, Special Publication 24. Cushman Foundation for Foraminiferal Research, Washington, DC, pp 137–149
- Ross CA, Ross JRP (1988) Late Paleozoic transgressive regressive deposition. In: Wilgus CK, Hastings BS, Kendall CGSC, Posamentier HW, Ross CA, Van Wagoner JC (eds) *Sea level change: an integrated approach*, Special Publication vol 42. Society of Economic Paleontologists and Mineralogists, Tulsa, pp 227–247
- Royer DL (2006) CO₂-forced climate thresholds during the Phanerozoic. *Geochim Cosmochim Acta* 70:5665–5675
- Scher HD, Martin EE (2006) Timing and climatic consequences of the opening of Drake Passage. *Science* 312:428–430
- Scherer CMS, Goldberg K (2007) Palaeowind patterns during the latest Jurassic-earliest Cretaceous in Gondwana: evidence from aeolian cross-strata of the Botucatu Formation, Brazil. *Palaeogeogr Palaeoclimatol Palaeoecol* 250(1–4):89–100
- Scotese CR (2001) Atlas of earth history. PALEOMAP Project, Arlington
- Scotese CR (2012) PALEOMAP, Earth history and climate history. [WWW document]. URL <http://www.scotese.com/>. Accessed Mar 2012
- Scotese CR, Summerhayes CP (1986) A computer model of paleoclimate to predict upwelling in the Mesozoic and Cenozoic. *Geobite* 1:28–42
- Sellwood BW, Valdes PJ (2006) Mesozoic climates: general circulation models and the rock record. *Sediment Geol* 190:269–287
- Sellwood BW, Valdes PJ, Price GD (2000) Geological evaluation of GCM simulations of Late Jurassic palaeoclimate. *Palaeogeogr Palaeoclimatol Palaeoecol* 156:147–160
- Sewall JO, van de Wal RSW, van der Zwan K, van Oosterhout C, Dijkstra HA, Scotese CR (2007) Climate model boundary conditions for four Cretaceous time slices. *Clim Past* 3:647–657
- Sijp WP, England MH (2004) Effect of the Drake Passage throughflow on global climate. *J Phys Oceanogr* 34:1254–1266

- Trenberth KE (1992) *Climate system modeling*. Cambridge University Press, New York, 788 p
- U.S. Geological Survey Geologic Names Committee (2010) Divisions of geologic time—major chronostratigraphic and geochronologic units: U.S. Geological Survey Fact Sheet 2010–3059, 2 p
- Valdes PJ (1993) Atmospheric general circulation models of the Jurassic. *Philos Trans R Soc B* 341(1297):317–326
- Valdes PJ (2000) Warm climate forcing mechanisms. In: Huber BT, MacLeod KG, Wing SL (eds) *Warm climates in earth history*. Cambridge University Press, Cambridge, pp 3–20
- Valdes PJ, Sellwood BW (1992) A palaeoclimate model for the Kimmeridgian. *Palaeogeogr Palaeoclimatol Palaeoecol* 95:47–72
- Veizer J, Ala D, Azmy K, Bruckschen P, Buhl D, Bruhn F, Carden GAF, Diener A, Ebner S, Godderis Y, Jasper T, Korte C, Pawellek F, Podlaha O, Strauss H (1999) $^{87}\text{Sr}/^{86}\text{Sr}$, $\delta^{13}\text{C}$ and $\delta^{18}\text{O}$ evolution of Phanerozoic seawater. *Chem Geol* 161:59–88
- Volkheimer W, Rauhut OWM, Quattrocchio ME, Martínez MA (2008) Jurassic Paleoclimates in Argentina, a review. *Rev Asoc Geol Argent* 63(4):549–556
- Walter H (1985) *Vegetation of the earth*. Springer, Berlin, 318 pp
- Ward PL (2009) Sulfur dioxide initiates global climate change in four ways. *Thin Solid Films* 517:3188–3203
- Winguth AME, Heinze C, Kutzbach JE, Maier-Reimer E, Mikolajewicz U, Rowley D, Rees A, Ziegler AM (2002) Simulated ocean circulation of the Middle Permian. *Paleoceanography* 17(5):1057
- Winterer EL (1991) The Tethyan Pacific during Late Jurassic and Cretaceous times. *Palaeogeogr Palaeoclimatol Palaeoecol* 87:253–265
- Zhou J, Poulsen CJ, Pollard D, White TS (2008) Simulation of modern and middle Cretaceous marine $\delta^{18}\text{O}$ with an ocean–atmosphere general circulation model. *Paleoceanography* 23, PA3223. doi:[10.1029/2008PA001596](https://doi.org/10.1029/2008PA001596)
- Ziegler PA (1988) *Evolution of the Arctic–North–Atlantic and the western Tethys*. American Association of Petroleum Geologists, Tulsa
- Ziegler AM, Scotese CR, Barrett SF (1982) In: Brosche F, Sundermann J (eds) *Tidal friction and earth's rotation II*. Springer, Berlin
- Ziegler AM, Gibbs MT, Hulver ML (1998) A mini-atlas of oceanic water masses in the Permian period. *Proc R Soc Aust* 110(1/2):323–343